



Host-Guest Interactions Between Metal–Organic Frameworks and Air-Sensitive Complexes at High Temperature

Bo Huang^{1,2*} and Zhe Tan¹

¹Institute of Chemical Engineering and Technology, Xi'an Jiaotong University, Xi'an, China, ²State Key Laboratory of Structural Chemistry, Fujian Institute of Research on the Structure of Matter, Chinese Academy of Sciences, Fuzhou, China

The host-guest chemistry of metal–organic frameworks (MOFs) has been attracting increasing attention owing to the outstanding properties derived from MOFs-guests combinations. However, there are large difficulties involved in the syntheses of the host-guest MOF systems with air-sensitive metal complexes. In addition, the behaviors on host-guest interactions in the above systems at high temperature are not clear. This study reported the synthetic methods for host-guest systems of metal–organic framework and air-sensitive metal complexes via a developed chemical vapor infiltration process. With the synchrotron X-ray powder diffraction (XRPD) measurements and Fourier Transform infrared spectroscopy (FTIR), the successful loadings of Fe(CO)₅ in HKUST-1 and NH₂-MIL-101(Al) have been confirmed. At high temperatures, the structural and chemical componential changes were investigated in detail by XRPD and FTIR measurements. HKUST-1 was proven to have strong interaction with Fe(CO)₅ and resulted in a heavy loading amount of 63.1 wt%, but too strong an interaction led to deformation of HKUST-1 sub-unit under heating conditions. NH₂-MIL-101(Al), meanwhile, has a weaker interaction and is chemically inert to Fe(CO)₅ at high temperatures.

Keywords: HKUST-1, MIL-101, Fe(CO)₅, chemical vapor infiltration, host-guest interaction, high temperature

OPEN ACCESS

Edited by:

Truc Kim Nguyen,
Vietnam National University, Vietnam

Reviewed by:

Xuan Zhang,
Donghua University, China
Dong-Sheng Guo,
Nankai University, China

*Correspondence:

Bo Huang
bohuang@xjtu.edu.cn

Specialty section:

This article was submitted to
Supramolecular Chemistry,
a section of the journal
Frontiers in Chemistry

Received: 08 May 2021

Accepted: 16 June 2021

Published: 03 August 2021

Citation:

Huang B and Tan Z (2021) Host-Guest Interactions Between Metal–Organic Frameworks and Air-Sensitive Complexes at High Temperature. *Front. Chem.* 9:706942. doi: 10.3389/fchem.2021.706942

INTRODUCTION

Metal–organic frameworks (MOFs) or porous coordination polymers (PCPs) have attracted much attention in the past several decades (Zhang et al., 2020; Yuan et al., 2018). Benefiting from their high crystallinity, porosity, and designability, thousands of unique MOFs have been designed and synthesized, with potential applications in gas storage (Chen et al., 2020; Tian et al., 2018; Kalmutzki, Diercks, and Yaghi 2018; Alezi et al., 2015; Jiang et al., 2016), separation (Fu et al., 2016; Liu et al., 2018; Gao et al., 2020; Peng et al., 2017; Zhang et al., 2019), catalysis (Wang, An, and Lin 2019; Liang et al., 2018; Manna et al., 2015), and so on. On the other hand, metal complexes are one of the most developed research fields, with various properties such as magnetism (Guo, Bar, and Layfield 2019), superconductivity (Wang et al., 2019), and catalysis (Nicastrì et al., 2020; Trammell, Rajabimoghadam, and Garcia-Bosch 2019). It would be useful to merge MOFs and metal complexes together and investigate their host-guest chemistry.

There have been several pioneering works in this field, but most research is focused on physical properties like electrical conductivity (Talin et al., 2014) and magnetism (Han et al., 2015). The interactions based on chemical properties between host MOFs and guest metal complexes are

relatively less researched (Nayak, Harms, and Dehnen 2011). The largest limitation on research of host-guest systems for MOFs and metal complexes is the difficulties in their syntheses, especially in air-sensitive systems. In chemical processes, the chemical components and structures of them may have complicated changes. The systematic investigation on the host-guest chemistry of MOF-metal complex systems with air-sensitive complexes has rarely been reported, although a few air-stable metal complexes have already been researched, such as FeCp₂ and Ru (cod) (cot) (Kalidindi, Yussenko, and Fischer 2011).

In this study, we reported a systematic research on MOF-metal complex systems of air-sensitive Fe(CO)₅ guest in HKUST-1 and NH₂-MIL-101(Al), consisting of syntheses, characterization, and investigation on host-guest interactions at high temperatures.

EXPERIMENTAL

Synthesis of HKUST-1

875 mg of Cu(NO₃)₂·3H₂O and 420 mg of benzene-1,3,5-tricarboxylic acid (BTC) were dissolved in 24 ml of H₂O and EtOH mixture solvent (1:1 vol. ratio). The solution was sealed in a solvothermal container and reacted at 120°C for 12 h. The solution was then cooled down to room temperature at a fixed rate for 6 h. The light blue solid was filtered and washed with EtOH. The washed HKUST-1 was dried at 60°C and activated at 100°C under vacuum. The activated sample was stored in a glovebox for further use.

Synthesis of NH₂-MIL-101(Al)

Aluminium chloride hexahydrate (AlCl₃·6H₂O, 0.51 g), 2-amino terephthalic acid (0.56 g), and DMF (30 ml) were heated at 130°C over 3 days. The product was refluxed in methanol overnight and dried at 100°C under vacuum overnight. The activated sample was stored in a glovebox for further use.

X-Ray Powder Diffraction and Synchrotron X-Ray Powder Diffraction

The crystal structures of MOFs, Fe(CO)₅-loaded MOFs, and their thermal decomposition products were investigated by powder XRD analysis using a Bruker D8 Advance diffractometer (Cu K α radiation).

The crystal structures were investigated by capillary synchrotron XRPD analysis measured at the BL02B2 beamline, SPring-8. The XRPD patterns of the samples sealed in a glass capillary were measured *in situ* with a wavelength of 1.000 Å.

Fourier Transform Infrared Spectroscopy and Transmission Electron Microscopy

FTIR spectra of MOFs, Fe(CO)₅-loaded MOFs, and their thermal decomposition products were obtained to evaluate sample structures. All IR spectra were recorded inside a glovebox using a Bruker PLATINUM ATR FTIR spectrometer, accumulating 64 scans at a resolution of 4 cm⁻¹.

TEM images were captured using Talos F200X operated at 200 kV accelerating voltage.

RESULTS AND DISCUSSION

Chemical Vapor Infiltration of Fe(CO)₅ Into HKUST-1

Fe(CO)₅ is one of the most common metal complexes which are sensitive to air. The Fe(CO)₅ loading experiment in HKUST-1 was shown in the schematic image of **Figure 1A** via a chemical vapor infiltration (CVI) method. The HKUST-1 was synthesized and activated according to the reported method (Chui et al., 1999). The as-synthesized HKUST-1 was confirmed by capillary XRPD measurement; similar XRPD patterns with simulated HKUST-1 proved the successful synthesis of HKUST-1 (**Supplementary Figure S1**).

104.5 mg of activated HKUST-1 and 405.3 mg Fe(CO)₅ were sealed in CVI vessel inside a glovebox (**Figure 1B** left). The CVI vessel was transferred to autoclave and heated at 60°C for 2 h for Fe(CO)₅ loading; the obtained product was named Fe(CO)₅@HKUST-1 (**Figure 1B** right). The mass of CVI product was weighed inside a glovebox as 270.3 mg, with 61.3 wt% loading amount.

To check the state of Fe(CO)₅ loading in HKUST-1, synchrotron XRPD measurements have been carried out with incident wavelengths of 1.000 Å. All samples were kept under inert conditions inside glass capillary during measurements. As shown in **Figure 2**, the activated HKUST-1 exhibits strong diffraction intensity. However, after loading with Fe(CO)₅, most of the diffraction peaks disappeared, with only remaining weak peaks below 10°. This phenomenon suggested the perturbation on the original crystalline structure of HKUST-1 by Fe(CO)₅ infiltration.

To further confirm the MOF structure after loading, FTIR measurements have been performed under inert conditions. As shown in **Supplementary Figure S2**, sharp IR peaks were observed in activated HKUST-1. After loading of Fe(CO)₅, all peaks originated from HKUST-1 remained, which strongly proved the stability of MOF structure before and after loading. In addition to those sharp peaks belonging to HKUST-1, a new typical carbonyl peak marked with asterisks has been found, confirming the successful loading of Fe(CO)₅. Furthermore, the red shift of HKUST-1 peak at 1,650 cm⁻¹ suggested the obstruction of MOF ligand vibration from the loaded Fe(CO)₅ guest molecules, which gave further proof for successful loading of Fe(CO)₅ inside HKUST-1 pores.

High Temperature Behavior of Fe(CO)₅@HKUST-1

In order to further understand the host-guest interactions between HKUST-1 and Fe(CO)₅, we performed high temperature experiments with different heating conditions inside a glovebox. As shown in **Supplementary Figure S3A**, the dark blue solid of Fe(CO)₅@HKUST-1 was heated at 140°C, and the color change to yellow was observed after 10 min heating

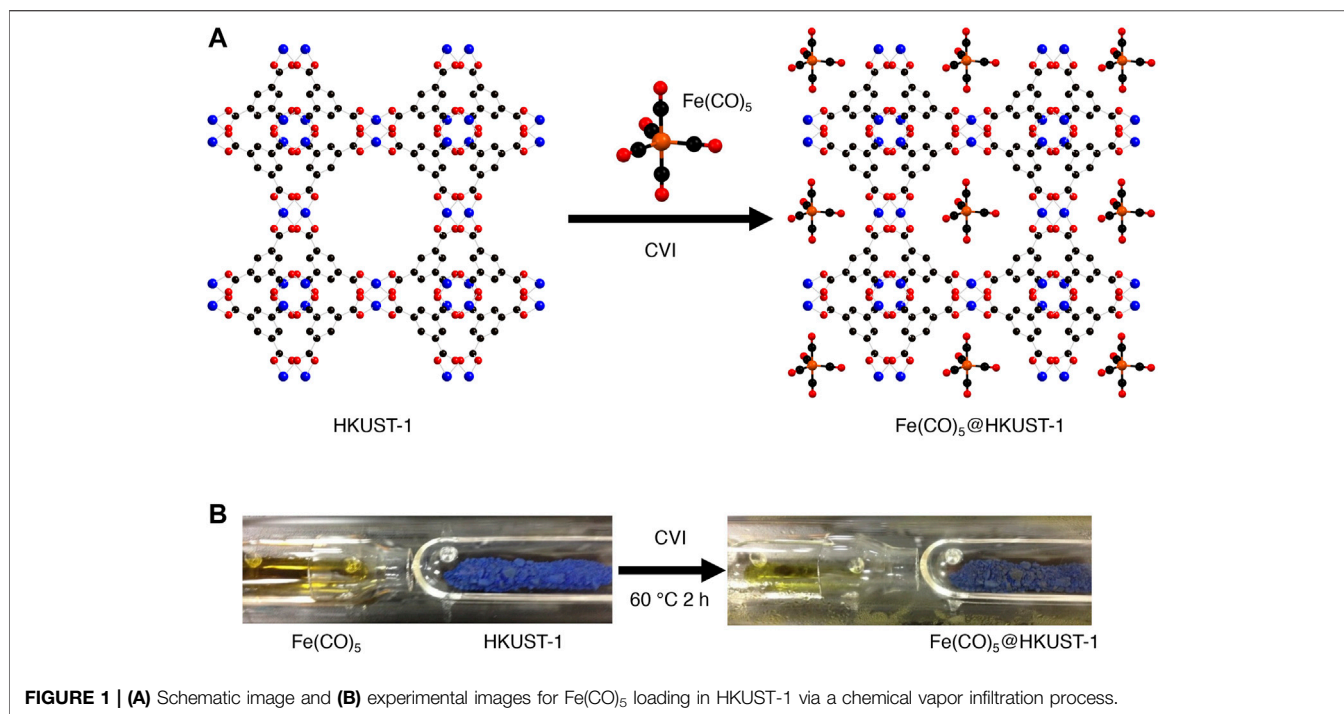


FIGURE 1 | (A) Schematic image and **(B)** experimental images for Fe(CO)₅ loading in HKUST-1 via a chemical vapor infiltration process.

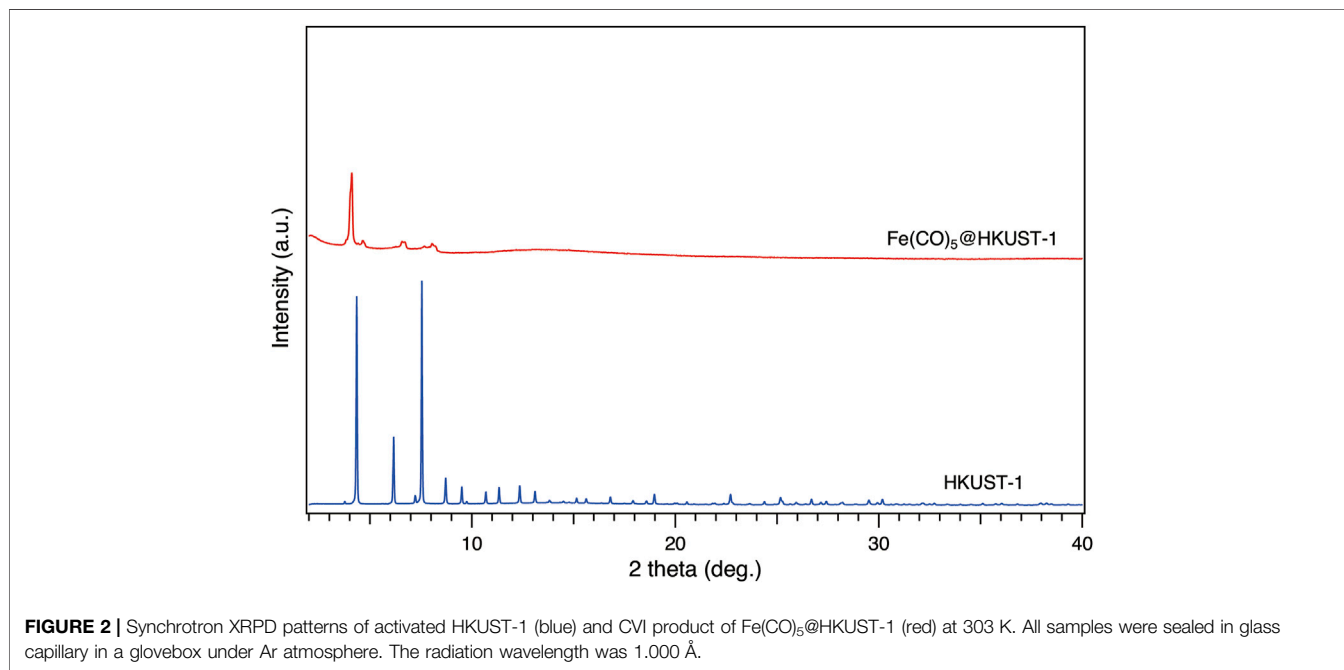


FIGURE 2 | Synchrotron XRPD patterns of activated HKUST-1 (blue) and CVI product of Fe(CO)₅@HKUST-1 (red) at 303 K. All samples were sealed in glass capillary in a glovebox under Ar atmosphere. The radiation wavelength was 1.000 Å.

(sample named **140-10**). We also tested other heating temperature of 170 and 200°C; similar color changes to yellow solid occurred within 1 min (**Supplementary Figure S3B**, samples named **170-1** and **200-1**, respectively). For longer heating times at 200°C, a gradual color change from yellow to purple was observed within 1.5 h (**Supplementary Figure S3B**, sample named **200-90**).

To explore the structural information of Fe(CO)₅@HKUST-1 under various heating conditions, we performed XRPD measurements under inert conditions by using an inert sample holder (**Supplementary Figure S4**). Before measurements, to avoid the samples being contaminated by air, the inert holder was tightly sealed inside a glovebox after sample setup. The measurement results are shown in **Figure 3**; after heat

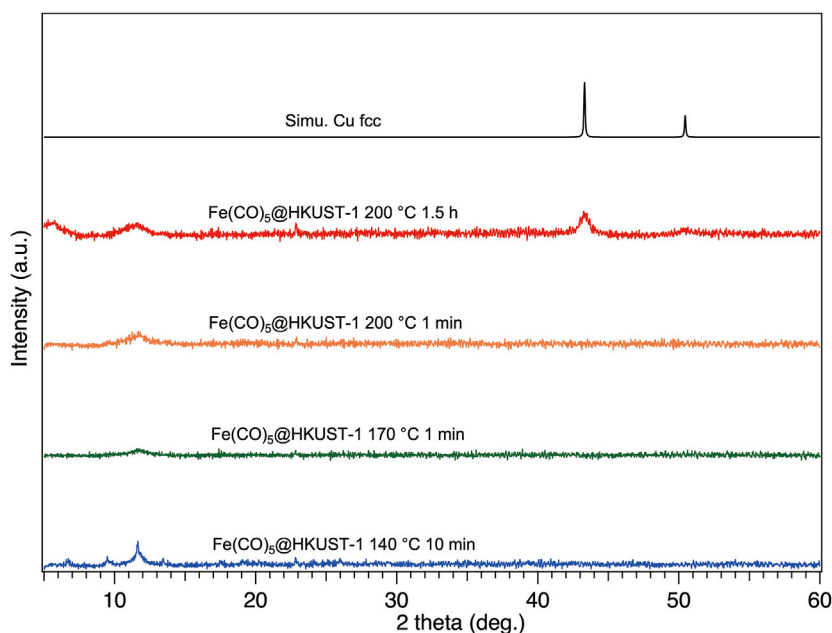


FIGURE 3 | XRPD patterns of Fe(CO)₅@HKUST-1 decomposed at different conditions: 140°C-10 min (blue), 170°C-1 min (green), 200°C-1 min (orange), 200°C-1.5 h (red), and simulated Cu (black). All samples were sealed inside a glovebox and measured under inert conditions. The background of XRPD patterns had been removed for clarity. The radiation wavelength was 1.5406 Å.

treatment at 140°C for 10 min, the crystallinity of HKUST-1 was slightly damaged compared with XRPD pattern of Fe(CO)₅@HKUST-1 in **Figure 2**, due to the thermal decomposition of Fe(CO)₅. In TEM image of **140-10**, a homogenous solid structure was observed (**Supplementary Figure S5**), the result is consistent with its XRPD pattern. For **170-1**, even the heating time was much shorter than **140-10**, and higher temperatures led to harsh damage on crystallinity, where only the (222) main peak at 11.8° of HKUST-1 remained, shown in **Figure 3**, owing to faster decomposition of Fe(CO)₅. The XRPD result of **200-1** was similar to that of **170-1** (**Figure 3**).

With the extension of heating time to 1.5 h (sample **200-90**), a crush of crystallinity was accompanied with the appearance of new broad diffraction peaks at 43.5 and 50.7°, which are consistent with diffraction peaks of simulated face-centered cubic (fcc) Cu, proving the generation of Cu NPs. Actually, under vacuum conditions, after heating at 200°C for 18 h, no Cu diffraction peak was detected (**Supplementary Figure S6**). Even with sufficient heating of HKUST-1 at 500°C for 2 h (Lee et al., 2019), instead of the metallic state of Cu NPs, only semiconductor CuO NPs can be obtained. On the other hand, Cu NPs can be easily generated when the heating atmosphere is changed to 1 atm of H₂, at 200°C for 1 h (**Supplementary Figure S7**). Under H₂ atmosphere, the decreasing on (222) peak of Cu²⁺ ion-rich plane in HKUST-1 and the increasing on (111) peak of Cu NPs demonstrate the migration of Cu elements from the square-planar coordinated Cu²⁺ ions in HKUST-1 to dodecahedral coordinated Cu atoms in fcc-Cu NPs. Therefore, in sample **200-90**, it may be suggested that the reduction reaction of Cu²⁺ to Cu atom was triggered by decomposition of Fe(CO)₅.

The existence of Cu NPs in **200-90** was also confirmed by TEM measurement (**Supplementary Figure S8**).

To understand more about the thermal decomposition processes of the Fe(CO)₅@HKUST-1 at various conditions, the FTIR spectroscopy has been measured inside a glovebox (**Figure 4**). Samples **140-10**, **170-1**, and **200-1** show almost identical IR spectra among each other. The incomplete decomposition of Fe(CO)₅ can be noticed from the remaining typical CO peaks in these three samples. The broadening of MOF peaks compared with the initial sharp peaks from HKUST-1 demonstrated the decomposition of MOFs sub-units under thermal decomposition of Fe(CO)₅ guest molecule, in addition to the collapse of HKUST-1 crystal structure confirmed by XRPD measurements in **Figure 3B**. In spectrum of **200-90**, CO peaks vanished because of the complete decomposition of Fe(CO)₅ with a longer heat treatment.

High Temperature Behavior of Fe(CO)₅@MIL-101(Al)

The above results have shown the host-guest interactions in case of Fe(CO)₅@HKUST-1 at high temperatures, where the decomposition of Fe(CO)₅ broke the Cu₂O₈ clusters in HKUST-1. Other MOFs with different clusters may resist Fe(CO)₅ at high temperatures. Among potential candidate MOFs, we guessed that NH₂-MIL-101(Al) can be durable to Fe(CO)₅ at high temperature because of its relatively high thermal stability and chemical inertness. The NH₂-MIL-101(Al) was synthesized via a reported protocol (Serra-Crespo et al., 2011).

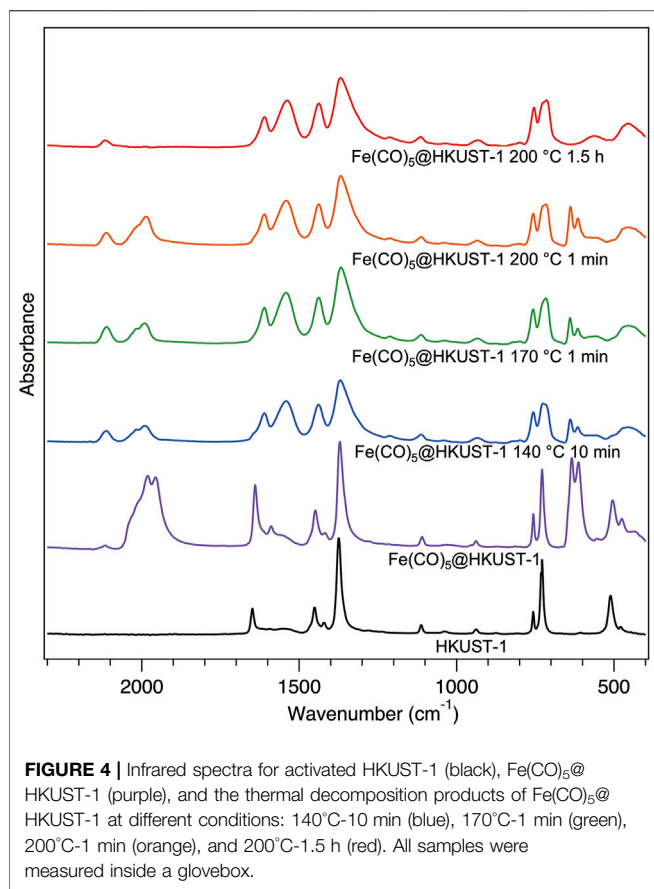


FIGURE 4 | Infrared spectra for activated HKUST-1 (black), Fe(CO)₅@HKUST-1 (purple), and the thermal decomposition products of Fe(CO)₅@HKUST-1 at different conditions: 140°C-10 min (blue), 170°C-1 min (green), 200°C-1 min (orange), and 200°C-1.5 h (red). All samples were measured inside a glovebox.

After activation of NH₂-MIL-101(Al), the gas phase loading of Fe(CO)₅ to NH₂-MIL-101(Al) was performed by CVI process under similar conditions. 101.7 mg of activated NH₂-MIL-101(Al) and 403.2 mg Fe(CO)₅ were kept at 60°C for 2 h under Ar atmosphere. The mass of loading product Fe(CO)₅@MIL-101(Al) was 127.4 mg with 20.2 wt% loading amount. Lower loading amounts for NH₂-MIL-101(Al) than 61.3 wt% of HKUST-1 may be attributed to its weaker host-guest interaction as the lack of open metal site.

The CVI product Fe(CO)₅@MIL-101(Al) was investigated by FTIR measurements performed inside the glovebox. As shown in **Figure 5A**, there are typical carbonyl vibration peaks in the spectrum of Fe(CO)₅@MIL-101(Al) marked with asterisks, proving the existence of Fe(CO)₅ guest molecules in the product. Combined with the carbonyl peaks, the sustenance for the IR peaks of the MOF structure before and after CVI process suggested the successful loading of Fe(CO)₅ to NH₂-MIL-101(Al) without breaking the MOF structure.

The thermal stability of Fe(CO)₅@MIL-101(Al) was tested under inert conditions. Fe(CO)₅@MIL-101(Al) was heated to 200°C (same temperature as Fe(CO)₅@HKUST-1) for 0.5 h, referred to as **200-30**. In **Figure 5A**, with the comparison of the FTIR spectra of NH₂-MIL-101(Al), Fe(CO)₅@MIL-101(Al), and **200-30**, the complete decomposition of Fe(CO)₅ and the maintaining of MOF structure can be confirmed in **200-30**. On the other hand, in XRPD measurement results shown in

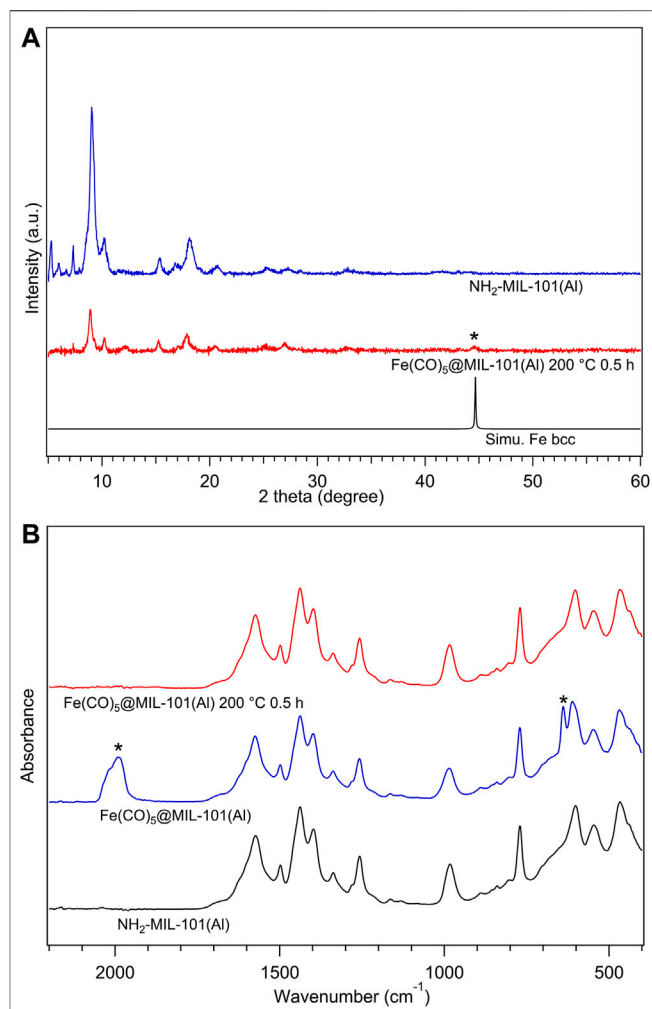


FIGURE 5 | (A) Infrared spectra for activated NH₂-MIL-101(Al) (black), Fe(CO)₅@MIL-101(Al) (blue), and Fe(CO)₅@MIL-101(Al) decomposed at 200°C/0.5 h (red), all samples were measured inside a glovebox. **(B)** XRPD patterns of NH₂-MIL-101(Al) (black), Fe(CO)₅@MIL-101(Al) decomposed at 200°C/0.5 h (red), and simulated body-centred-cubic Fe (black), all samples were measured under inert conditions by capillary technique. The radiation wavelength was 1.5406 Å.

Figure 5B, the asterisk diffraction peak from the body-centred cubic (bcc) Fe NPs was detected in **200-30**, as solid evidence for Fe formation from Fe(CO)₅. The XRPD measurements also show the lower crystallinity in diffraction pattern of **200-30** compared with that of NH₂-MIL-101(Al), which may be considered as a perturbation of periodic structure by randomly dispersed guest molecules inside pores.

Finally, to elucidate the reasons for the different behaviors between Fe(CO)₅@HKUST-1 and Fe(CO)₅@MIL-101(Al), the possible reaction mechanisms in each case should be further discussed. Since the decomposition of Fe(CO)₅ below 150°C is negligible (Carlton and Oxley, 1965), the molecular Fe(CO)₅ reacting with HKUST-1 backbone in **140-10** can be considered as the redox reaction between penta-coordinated Fe (0) with tetra-coordinated Cu(II) open metal sites. At

higher temperatures of 170 and 200°C, the Fe(CO)₅ decompositions were significantly promoted, supplying atomic Fe and molecular CO to these systems. HKUST-1 backbone is stable with CO molecule to at least 210°C, (Stawowy et al., 2020), therefore, the rapid destruction of MOFs shown in **Figure 4** for **170-1** and **200-1** are mainly attributed to the strong reduction ability of atomic Fe. As the ligand reactivity difference between benzene-1,3,5-tricarboxylic acid in HKUST-1 and 2-amino terephthalic acid in NH₂-MIL-101(Al) is almost negligible, the main reason for the different behavior of Fe(CO)₅@HKUST-1 and Fe(CO)₅@MIL-101(Al) can be concluded as the different reactivity of metal ions. With the systematic investigations on loading and heating processes of Fe(CO)₅ guest to HKUST-1 and NH₂-MIL-101(Al), the interactions between host MOFs and guest molecules were clarified.

CONCLUSION

The host-guest systems of MOFs and air-sensitive metal complexes were synthesized, with Fe(CO)₅ loaded in HKUST-1 and NH₂-MIL-101(Al) via a chemical vapor infiltration process. With the XRPD and FTIR measurements under inert conditions, the successful loading of Fe(CO)₅ in HKUST-1 and NH₂-MIL-101(Al) has been confirmed. The interactions between MOFs and Fe(CO)₅ at different heating temperatures were investigated in detail. As a result, the Fe(CO)₅@HKUST-1 was not stable under thermal conditions. Under minor heating conditions, deconstructions of HKUST-1 sub-unit were observed from XRPD and FTIR results; under major heating conditions, Cu²⁺ ions in HKUST-1 were reduced to Cu NPs with the interaction to Fe(CO)₅. On the other hand, in Fe(CO)₅@MIL-101(Al), the decomposition of Fe(CO)₅ to Fe NPs was found and NH₂-MIL-101(Al) was stable to Fe(CO)₅ as well as its decomposition products. The synthetic methods and the systematic investigation for the air-sensitive host-guest MOFs-metal complex systems in this report provide valuable experimental experience and insight between porous functional materials and

REFERENCES

- Alezi, D., Belmabkhout, Y., Suyetin, M., Bhatt, P. M., Weseliński, Ł. J., Solovyeva, V., et al. (2015). MOF Crystal Chemistry Paving the Way to Gas Storage Needs: Aluminum-Based Soc-MOF for CH₄, O₂, and CO₂ Storage. *J. Am. Chem. Soc.* 137, 13308–13318. doi:10.1021/jacs.5b07053
- Carlton, H. E., and Oxley, J. H. (1965). Kinetics of the Heterogeneous Decomposition of Iron Pentacarbonyl. *Aiche J.* 11, 79–84. doi:10.1002/aic.690110119
- Chen, Z., Li, P., Anderson, R., Wang, X., Zhang, X., Robison, L., et al. (2020). Balancing Volumetric and Gravimetric Uptake in Highly Porous Materials for Clean Energy. *Science* 368, 297–303. doi:10.1126/science.aaz8881
- Chui, S. S., Lo, S. M. F., Charmant, J. P. H., Orpen, A. G., and Williams, I. D. (1999). A Chemically Functionalizable Nanoporous Material [Cu₃(TMA)₂(H₂O)₃]_n. *Science* 283, 1148–1150. doi:10.1126/science.283.5405.1148
- Fu, J., Das, S., Xing, G., Ben, T., Valtchev, V., and Qiu, S. (2016). Fabrication of COF-MOF Composite Membranes and Their Highly Selective Separation of H₂/CO₂. *J. Am. Chem. Soc.* 138, 7673–7680. doi:10.1021/jacs.6b03348
- Gao, J., Qian, X., Lin, R. B., Krishna, R., Wu, H., Zhou, W., et al. (2020). Mixed Metal-Organic Framework with Multiple Binding Sites for Efficient C₂H₂/CO

guest molecules. We envision that this method could be expanded to other metal precursors and porous materials on fabricating various functional nanocomposites and devices.

DATA AVAILABILITY STATEMENT

The original contributions presented in the study are included in the article/**Supplementary Material**, further inquiries can be directed to the corresponding author.

AUTHOR CONTRIBUTIONS

BH has designed the work and performed the experiments. BH and ZT cowrote the manuscript.

FUNDING

This research was supported by the Fundamental Research Fund of Xi'an Jiaotong University, xxj032019005, the fellowship of China Postdoctoral Science Foundation 2020M673370, National Natural Science Foundation of China 22001202, and State Key Laboratory of Structural Chemistry open fund 20200032.

ACKNOWLEDGMENTS

Acknowledgment to my colleagues Qingyuan Yang and his student Yongli Dong for their kind help on XRPD measurements.

SUPPLEMENTARY MATERIAL

The Supplementary Material for this article can be found online at: <https://www.frontiersin.org/articles/10.3389/fchem.2021.706942/full#supplementary-material>

2 Separation. *Angew. Chem. Int. Ed.* 59, 4396–4400. doi:10.1002/anie.202000323

Guo, F.-S., Bar, A. K., and Layfield, R. A. (2019). Main Group Chemistry at the Interface with Molecular Magnetism. *Chem. Rev.* 119, 8479–8505. doi:10.1021/acs.chemrev.9b00103

Han, S., Kim, H., Kim, J., and Jung, Y. (2015). Modulating the Magnetic Behavior of Fe(II)-MOF-74 by the High Electron Affinity of the Guest Molecule. *Phys. Chem. Chem. Phys.* 17, 16977–16982. doi:10.1039/c5cp01441g

Jiang, J., Furukawa, H., Zhang, Y.-B., and Yaghi, O. M. (2016). High Methane Storage Working Capacity in Metal-Organic Frameworks with Acrylate Links. *J. Am. Chem. Soc.* 138, 10244–10251. doi:10.1021/jacs.6b05261

Kalidindi, S. B., Yussenko, K., and Fischer, R. A. (2011). Metallocenes@COF-102: Organometallic Host-Guest Chemistry of Porous Crystalline Organic Frameworks. *Chem. Commun.* 47, 8506–8508. doi:10.1039/c1cc11450f

Kalmutzki, M. J., Diercks, C. S., and Yaghi, O. M. (2018). Metal-Organic Frameworks for Water Harvesting from Air. *Adv. Mater.* 30, 1704304. doi:10.1002/adma.201704304

Lee, J. E., Kim, D. Y., Lee, H.-K., Park, H. J., Ma, A., Choi, S.-Y., et al. (2019). Sonochemical Synthesis of HKUST-1-Based CuO Decorated with Pt Nanoparticles for Formaldehyde Gas-Sensor Applications. *Sensors Actuators B: Chem.* 292, 289–296. doi:10.1016/j.snb.2019.04.062

- Liang, Z., Qu, C., Xia, D., Zou, R., and Xu, Q. (2018). Atomically Dispersed Metal Sites in MOF-Based Materials for Electrocatalytic and Photocatalytic Energy Conversion. *Angew. Chem. Int. Ed.* 57, 9604–9633. doi:10.1002/anie.201800269
- Liu, G., Chernikova, V., Liu, Y., Zhang, K., Belmabkhout, Y., Shekha, O., et al. (2018). Mixed Matrix Formulations with MOF Molecular Sieving for Key Energy-Intensive Separations. *Nat. Mater.* 17, 283–289. doi:10.1038/s41563-017-0013-1
- Manna, K., Zhang, T., Greene, F. X., and Lin, W. (2015). Bipyridine- and Phenanthroline-Based Metal-Organic Frameworks for Highly Efficient and Tandem Catalytic Organic Transformations via Directed C-H Activation. *J. Am. Chem. Soc.* 137, 2665–2673. doi:10.1021/ja512478y
- Nayak, S., Harms, K., and Dehnen, S. (2011). New Three-Dimensional Metal-Organic Framework with Heterometallic [Fe-Ag] Building Units: Synthesis, Crystal Structure, and Functional Studies. *Inorg. Chem.* 50, 2714–2716. doi:10.1021/ic1019636
- Nicastro, M. C., Lehnher, D., Lam, Y.-h., Dirocco, D. A., and Rovis, T. (2020). Synthesis of Sterically Hindered Primary Amines by Concurrent Tandem Photoredox Catalysis. *J. Am. Chem. Soc.* 142, 987–998. doi:10.1021/jacs.9b10871
- Peng, Y., Li, Y., Ban, Y., and Yang, W. (2017). Two-Dimensional Metal-Organic Framework Nanosheets for Membrane-Based Gas Separation. *Angew. Chem. Int. Ed.* 56, 9757–9761. doi:10.1002/anie.201703959
- Serra-Crespo, P., Ramos-Fernandez, E. V., Gascon, J., and Kapteijn, F. (2011). Synthesis and Characterization of an Amino Functionalized MIL-101(Al): Separation and Catalytic Properties. *Chem. Mater.* 23, 2565–2572. doi:10.1021/cm103644b
- Stawowy, M., Jagódka, P., Matus, K., Samojeden, B., Silvestre-Albero, J., Trawczyński, J., et al. (2020). HKUST-1-Supported Cerium Catalysts for CO Oxidation. *Catalysts* 10, 108. doi:10.3390/catal10010108
- Talin, A. A., Centrone, A., Ford, A. C., Foster, M. E., Stavila, V., Haney, P., et al. (2014). Tunable Electrical Conductivity in Metal-Organic Framework Thin-Film Devices. *Science* 343, 66–69. doi:10.1126/science.1246738
- Tian, T., Zeng, Z., Vulpe, D., Casco, M. E., Divitini, G., Midgley, P. A., et al. (2018). A Sol-Gel Monolithic Metal-Organic Framework with Enhanced Methane Uptake. *Nat. Mater.* 17, 174–179. doi:10.1038/NMAT5050
- Trammell, R., Rajabimoghadam, K., and Garcia-Bosch, I. (2019). Copper-Promoted Functionalization of Organic Molecules: from Biologically Relevant Cu/O₂ Model Systems to Organometallic Transformations. *Chem. Rev.* 119, 2954–3031. doi:10.1021/acs.chemrev.8b00368
- Wang, C., An, B., and Lin, W. (2019). Metal-Organic Frameworks in Solid-Gas Phase Catalysis. *ACS Catal.* 9, 130–146. doi:10.1021/acscatal.8b04055
- Wang, R.-S., Chen, L.-C., Yang, H., Fu, M.-A., Cheng, J., Wu, X.-L., et al. (2019). Superconductivity in an Organometallic Compound. *Phys. Chem. Chem. Phys.* 21, 25976–25981. doi:10.1039/c9cp04227j
- Yuan, S., Feng, L., Wang, K., Pang, J., Bosch, M., Lollar, C., et al. (2018). Stable Metal-Organic Frameworks: Design, Synthesis, and Applications. *Adv. Mater.* 30, 1704303. doi:10.1002/adma.201704303
- Zhang, C., Wu, B.-H., Ma, M.-Q., Wang, Z., and Xu, Z.-K. (2019). Ultrathin Metal/Covalent-Organic Framework Membranes towards Ultimate Separation. *Chem. Soc. Rev.* 48, 3811–3841. doi:10.1039/c9cs00322c
- Zhang, X., Chen, Z., Liu, X., Hanna, S. L., Wang, X., Taheri-Ledari, R., et al. (2020). A Historical Overview of the Activation and Porosity of Metal-Organic Frameworks. *Chem. Soc. Rev.* 49, 7406–7427. doi:10.1039/d0cs00997k

Conflict of Interest: The authors declare that the research was conducted in the absence of any commercial or financial relationships that could be construed as a potential conflict of interest.

Publisher's Note: All claims expressed in this article are solely those of the authors and do not necessarily represent those of their affiliated organizations, or those of the publisher, the editors and the reviewers. Any product that may be evaluated in this article, or claim that may be made by its manufacturer, is not guaranteed or endorsed by the publisher.

Copyright © 2021 Huang and Tan. This is an open-access article distributed under the terms of the Creative Commons Attribution License (CC BY). The use, distribution or reproduction in other forums is permitted, provided the original author(s) and the copyright owner(s) are credited and that the original publication in this journal is cited, in accordance with accepted academic practice. No use, distribution or reproduction is permitted which does not comply with these terms.